Effect of electric field on the rheological and dielectric properties of a liquid crystal exhibiting nematic–to–smectic-A phase transition

J. Ananthaiah, M. Rajeswari, V.S.S. Sastry, R. Dabrowski and S. Dhara

EDP SCIENCES   Società Italiana di Fisica   Springer

Regular Article

Effect of electric field on the rheological and dielectric properties of a liquid crystal exhibiting nematic–to–smectic-**A** phase transition

J. Ananthaiah[1], M. Rajeswari[1], V.S.S. Sastry[1], R. Dabrowski[2], and S. Dhara[1,a]

[1] School of Physics, University of Hyderabad, Hyderabad-500046, India
[2] Military University of Technology, Warsaw, Poland

Abstract. We report simultaneous measurements of shear viscosity (η) and dielectric constant (ϵ) of octyloxy cyanobiphenyl (8OCB) in the nematic (N) and smectic-A (SmA) phases as functions of temperature and electric field. With increasing electric field η increases in the N phase whereas it decreases in the SmA phase and saturates beyond a particular field in both the phases. The flow curves in the intermediate-field range show two Newtonian regimes in the N phase. The temperature-dependent behavior of η and ϵ at zero or at small electric field suggests the occurrence of several structures that results from precessional motion of the director along the neutral direction as reported in similar other system. We show that the precessional motions are gradually suppressed with increasing electric field and the effective viscosity resembles with the Miesowicz viscosity η_1 at high enough electric field. In the intermediate field range the temperature-dependent η exhibits anomalous behavior across the N-SmA phase transition which is attributed to the large contribution of Leslie coefficient α_1.

1 Introduction

Structure property relation, phase transitions and electro-optic properties of low-molecular-weight thermotropic liquid crystals have always been the main interest of scientists and technologists working in this area with the goal to achieve better liquid-crystal display (LCDs) properties. Flow behavior of such materials has not been studied so rigorously as it is not directly related to the device properties. Nevertheless some significant progress is made in understanding the flow behavior of low-molecular-weight liquid crystals both theoretically and experimentally [1–35]. Among them there are many reports on the measurement of Miesowicz viscosities or Leslie coefficients in the nematic phase as a function of temperature using various experimental techniques and the results are discussed on the basis of Leslie [1] and Ericksen [2] theories. However, the temperature-dependent shear viscosity is very different and complex in compounds exhibiting N-SmA phase transition. In a pioneering work Safinya *et al.* [14] have shown several steady-state structures that results from the interplay between the viscous frictional forces and flow-induced fluctuation forces by synchrotron X-ray radiation. They showed various shear-induced structural changes and precessional motions of nematic director in

the octyl cyanobiphenyl (8CB) compound as the SmA phase is approached.

In the nematic phase under shear there are mainly three different director orientations, namely a, b, c with respect to the flow (velocity) direction, and the corresponding Miesowicz viscosities [4] are represented by η_3, η_2 and η_1, respectively in fig. 1. In case of compounds having SmA phase the molecules form layered structures and the corresponding layer orientations are indicated as a', b' and c' in fig. 1. For all nematic liquid crystals $\alpha_2 < 0$ and the director orientation under flow depends on the sign of α_3. Normally near nematic-to-isotropic transition (T_{NI}) $\alpha_3 < 0$ and the ratio of Leslie coefficients α_2/α_3 is positive and the director tends to align along the flow direction with the orientation angle $\theta = \tan^{-1}\left(\sqrt{\alpha_2/\alpha_3}\right)$ with respect to the velocity direction. On the other hand α_3 is renormalized ($\alpha_3^R > 0$) in compounds exhibiting N-SmA transition due to the pretransitional smectic fluctuations and the flow alignment of the director is prohibited that leads to several structures namely $a_m, a_s, a(b)$ and a_c depending on the temperature and shear rate [14]. These structures arise because of precessional motion of the director along the neutral direction (x-axis) that can be described by the equation of an ellipse: $n_y^2(t)/n_{y0}^2 + n_z^2(t)/n_{z0}^2 = 1$, where $n_y(t) = n_{y0}\cos(\omega_0 t)$ and $n_z(t) = n_{z0}\sin(\omega_0 t)$ are components of the director $\mathbf{n}(t) = (n_x(t), n_y(t), n_z(t))$. Thus the director is precessing with an angular frequency
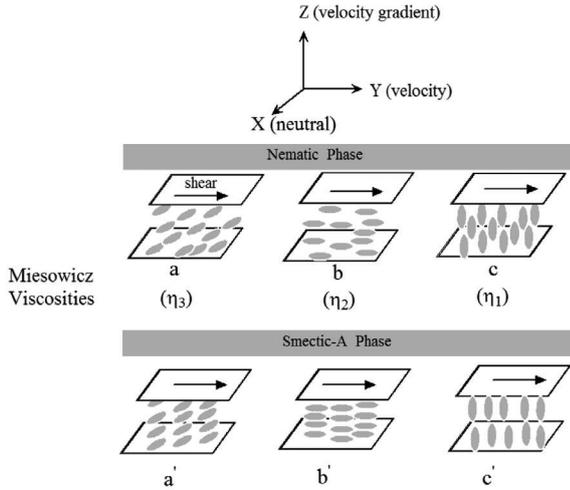
Fig. 1. Schematic representation of the three fundamental director orientations in the N and SmA phase under shear. The director orientations are along the x (neutral), y (velocity) and z (velocity gradient) directions in a, b, c, respectively. Layer orientations in the SmA phase are parallel to the zy, xz, and xy planes in a', b', and c', respectively. Miesowicz viscosities corresponding to each orientations in the N phase are designated by η_3, η_2 and η_1, respectively.

$\omega_0 = \sqrt{\dot{\gamma}^2(-\alpha_2\alpha_3^R)/\gamma_1^2}$ where α_3^R is the renormalized viscosity coefficient, $\dot{\gamma}$ is the shear rate and $\gamma_1 = \alpha_3 - \alpha_2$ [14]. The above-mentioned structures are described as follows. In a_m structure: the precessional motion is anisotropic with larger amplitude in the y-direction than in the z-direction ($n_{y0} > n_{z0}$); a_s structure: isotropic precession with equal amplitude in both the directions ($n_{y0} = n_{z0}$); $a(b)$ structure: anisotropic precession with lesser amplitude in the y-direction than in the z-direction ($n_{y0} < n_{z0}$) and in a_c structure: anisotropic precession with very large amplitude in the z-direction ($n_{y0} \ll n_{z0}$). The effect of these precessional motions are also reflected in the rheodielectric measurements [19]. In this paper we present electrorheological and rheodielectric studies on 8OCB and report the following experimental results: i) in the nematic phase the shear viscosity increases with increasing electric field in the low-shear-rate region and saturates at higher fields, ii) in the SmA phase the shear viscosity decreases with increasing electric field, iii) the precessional motions of the director just above the N-SmA transition under zero electric field appears to be similar as reported in 8CB [19] and in addition the precessional motions are suppressed at higher fields, iv) an anomalous peak appears in the shear viscosity under moderate electric field across the N-SmA transition that is suppressed at further higher fields.

2 Experimental

The compound 4'-octyloxy-4-cyanobiphenyl (8OCB) was synthesized in our laboratory, and exhibits the following phase sequences as observed in polarising optical microscope on cooling: I 79.5 °C N 66.6 °C SmA 54.5 °C
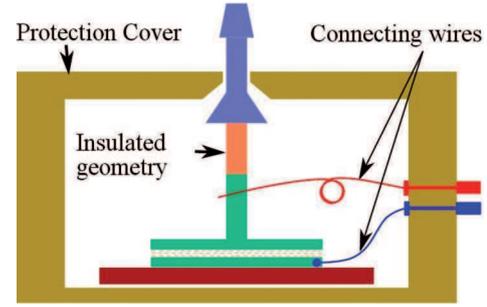
Fig. 2. (Color online) Schematic representation of the parallel-plate setup for simultaneous measurement of rheological and dielectric properties.

Cr. Rheological measurements were performed using a Rheometer (Anton Paar MCR 501) in parallel-plate geometry with plate diameter of 50 mm. The parallel-plate configuration was chosen for the simultaneous measurements of the rheological and dielectric properties. The cell gap was taken to be 75 μm as we experimentally verified that the effect of surface anchoring is observed below 50 μm. A similar observation was also reported by Cidade *et al.* [36]. In addition, we find that the zero-field viscosity in the isotropic and nematic phases of the same compound agrees well with the values reported in the literature in which the measurements are made by using other geometries [19,22]. A schematic setup for measuring the rheological and dielectric properties is shown in fig. 2. The electric field was applied between the bottom and the top plates by using a low-friction spring wire (fig. 2). The "air correction" *i.e.*, contribution due to the small friction in the absence of the sample was subtracted from the measured viscosity with the sample at various temperatures and fields. The dielectric constant was measured by measuring the ratio of the sample capacitance with that of the empty capacitance (*i.e.*, without sample). The temperature of the sample was controlled within an accuracy of 0.1 °C by a Peltier temperature controller fitted with a hood (protection cover) for the uniformity of the sample temperature. Calibration of the temperature controller was checked by measuring the phase transition temperatures of some standard liquid crystalline materials. All the measurements were made on cooling the sample from the isotropic phase. The dielectric properties were measured as a function of temperature up to 20 V with the help of a LCR meter (Agilent E4980A). To apply a voltage beyond 20 V we used a signal generator (Tektronix AFG3102) and a voltage amplifier (TEGAM). The frequency of the sinusoidal voltage was 3.11 kHz.

3 Results and discussion

The flow curve *i.e.* the variation of shear viscosity (η) as a function of shear rate ($\dot{\gamma}$) at various applied electric fields in the nematic phase (72 °C) is shown in fig. 3. The electric field is perpendicular (z-axis) to the flow field direction (y-axis in fig. 1). At zero field the viscosity is low (~ 10.5 mPa s) and is comparable to the shear viscosity η_3 [22]. It does not depend on the shear rate thus
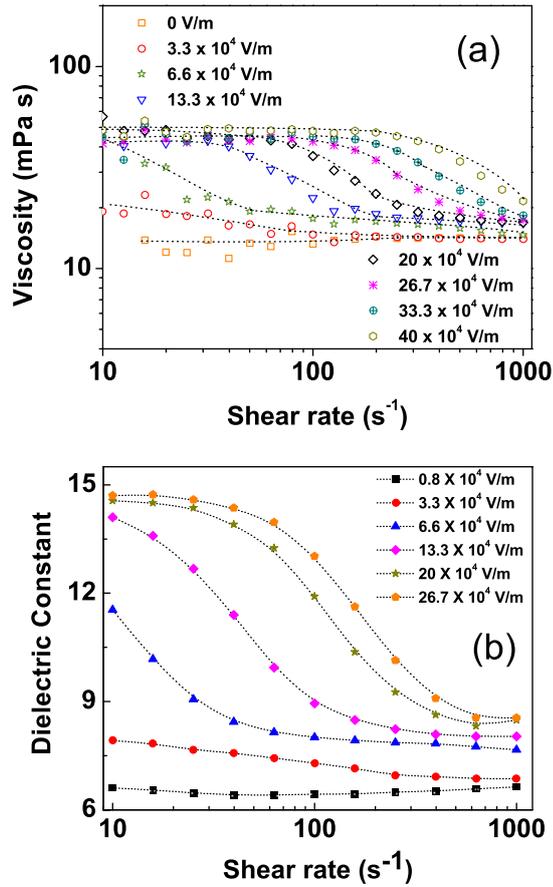
Fig. 3. (Color online) Variation of (a) shear viscosity (η) and (b) dielectric constant (ϵ) as a function of shear rate ($\dot{\gamma}$) at various applied ac electric fields. Dotted lines are drawn as a guide to the eye.

Fig. 4. (Color online) (a) Variation of the shear viscosity (η) as a function of applied electric field at various shear rates $\dot{\gamma}$ at $72\,^{\circ}$C. (b) Variation of the dielectric constant (ϵ) as a function of applied electric field at shear rates $\dot{\gamma} = 0$ and $50\,\mathrm{s}^{-1}$ at the same temperature. Dotted lines are drawn as a guide to the eye.

shows Newtonian flow behavior. With increasing electric field the director tends to align along the field direction beyond a threshold field as the dielectric anisotropy is positive ($\Delta\epsilon = \epsilon_{\parallel} - \epsilon_{\perp} > 0$). Both η (fig. 3(a)) and ϵ (fig. 3(b)) increase with increasing field up to $\sim 27 \times 10^4\,\mathrm{V/m}$ in the low-shear-rate region. At higher shear rate the flow field is strong and tends to align the director parallel to the xy-plane (fig. 1) as a result both η and ϵ decrease. In the intermediate shear rate a non-Newtonian flow behavior is observed where the director makes an angle with respect to the xy-plane due to the competition between the electric and the flow fields. Further beyond $\sim 6.6 \times 10^4\,\mathrm{V/m}$ viscosity shows two Newtonian regimes within the measured shear rate range. In the low-shear-rate region (up to $\dot{\gamma} \sim 100\,\mathrm{s}^{-1}$) there is no significant increase in η and ϵ beyond $\sim 27 \times 10^4\,\mathrm{V/m}$ suggesting that the director orientation is almost parallel to the electric field (z-axis). Furthermore, the shear rate at which the director orientation deviates from the electric field direction increases almost linearly with increasing field as seen in fig. 1 demonstrating the opposite and competing orientating effect of the flow field and electric field.

Variation of the shear viscosity with the applied electric field at different shear rates is shown in fig. 4(a). At shear rate $\dot{\gamma} \sim 50\,\mathrm{s}^{-1}$, the viscosity increases monotonically and saturates at higher field. No clear threshold is observed in the viscosity data as the director is already tilted by a finite angle with respect to the xy-plane. At higher shear rates ($\dot{\gamma} = 100$ and $199.5\,\mathrm{s}^{-1}$) in the intermediate-field region, *i.e.* from $\sim 8 \times 10^4\,\mathrm{V/m}$ to $\sim 30 \times 10^4\,\mathrm{V/m}$ (fig. 4(a)), η is always low compared to the values at $\dot{\gamma} = 50\,\mathrm{s}^{-1}$, suggesting that the tilt angle is reduced with respect to the xy-plane at higher shear rates. Beyond $\sim 30 \times 10^4\,\mathrm{V/m}$ the viscosity curves tend to saturate and merge together at higher field. There is a slight change in the slope of the viscosity at $\sim 8 \times 10^4\,\mathrm{V/m}$ (fig. 4(a)) and it can be explained as follows: The director gets partially aligned (homogeneously) due to the flow field and the slope change indicates a threshold field in the homogeneously aligned sample at which the director starts tilting significantly. Simultaneous measurement of the dielectric constant at the same temperature ($72\,^{\circ}$C) and at shear rate $\dot{\gamma} = 50\,\mathrm{s}^{-1}$ is shown in fig. 4(b). In the unsheared sample ($\dot{\gamma} = 0\,\mathrm{s}^{-1}$) the dielectric constant remains constant up to the threshold electric field $\sim 1.5 \times 10^4\,\mathrm{V/m}$ and then increases rapidly to saturate beyond $\sim 7 \times 10^4\,\mathrm{V/m}$. The dielectric constant below the threshold field is $\epsilon \sim 11$ and comparatively larger than measured in the aligned cell ($\epsilon_{\perp} \sim 7.3$ [29]) suggesting that the director orientation

is random in the unsheared sample. The dielectric constant at high field ($\sim 25 \times 10^4$ V/m) is comparable to $\epsilon_\parallel \sim 15.2$ [29] (measured in the aligned cell) and suggests that the director is oriented almost parallel to the field direction in the unsheared sample. At shear rate $\dot{\gamma} = 50\,\mathrm{s}^{-1}$, the dielectric data is very different than in the unsheared sample (fig. 4(b)). The dielectric constant is low ($\epsilon \sim 7.6$) compared to the unsheared sample indicating that the director is oriented slightly out of the xy-plane. The dielectric constant increases almost linearly up to $\sim 8 \times 10^4$ V/m and saturates at higher field followed by a slope change at this field and is consistent with the viscosity data in fig. 4(a).

The variation of temperature-dependent shear viscosity and the simultaneous measurement of the dielectric constant at various applied electric fields is shown in fig. 5. The viscosity does not depend on the electric field in the isotropic phase and is comparable to the previously reported values [22]. The rheodielectric [19] and shear-dependent X-ray measurements [15] of 8CB are suggestive for understanding the present temperature-dependent electrorheological and rheodielectric data of 8OCB. In the nematic phase the zero-field viscosity decreases initially up to $T - T_{NI} = -2°$ and suggests flow-induced alignment of the director (similar to the b orientation in fig. 1). Below this temperature a mixed state, namely a-b orientation, occurs and the viscosity increases monotonically up to $T - T_{NI} = -11°$ (fig. 5(a)). A slight slope change below this temperature followed by a rapid increase of the viscosity in the SmA phase is observed. The temperature-dependent dielectric constant (fig. 5(b)) together with the viscosity data between $T - T_{NI} = -11°$ and $-13°$ reflect the various precessional motions of the director along the neutral direction such as $a_c, a(b), a_s, a_m$ of the director that are seen in the X-ray measurements of the similar compound 8CB. In the SmA phase the viscosity is high due to the occurrence of the a'-c' orientation (fig. 1). When the field is increased to 13.3×10^4 V/m, the viscosity increases in the nematic phase and its temperature dependence is different than the zero-field viscosity. The temperature-dependent dielectric constant (fig. 5(b)) at this field in the nematic phase is higher compared to the values measured at smaller field (1.2×10^4 V/m) and indicates that the director is tilted with respect to the field direction. However, in the SmA phase the viscosity at 13.3×10^4 V/m is comparable to the zero-field viscosity, suggesting that this field is not sufficient to change the director orientation compared to the zero-field orientation. An anomalous increase in the viscosity is also observed across the N-SmA phase transition that will be discussed later. The dielectric constant (at 13.3×10^4 V/m) is rapidly increasing across the I-N transition and then decreases monotonically as the temperature is reduced towards the N-SmA transition. The temperature-dependent viscosity and the dielectric constant (fig. 5(a) and (b)) at this field just above the N-SmA transition does not show any signature of the presence of several structures as seen at zero field. Further, a comparatively smoother decrease of the dielectric constant and the increase of viscosity at 13.3×10^4 V/m with temperature in the nematic
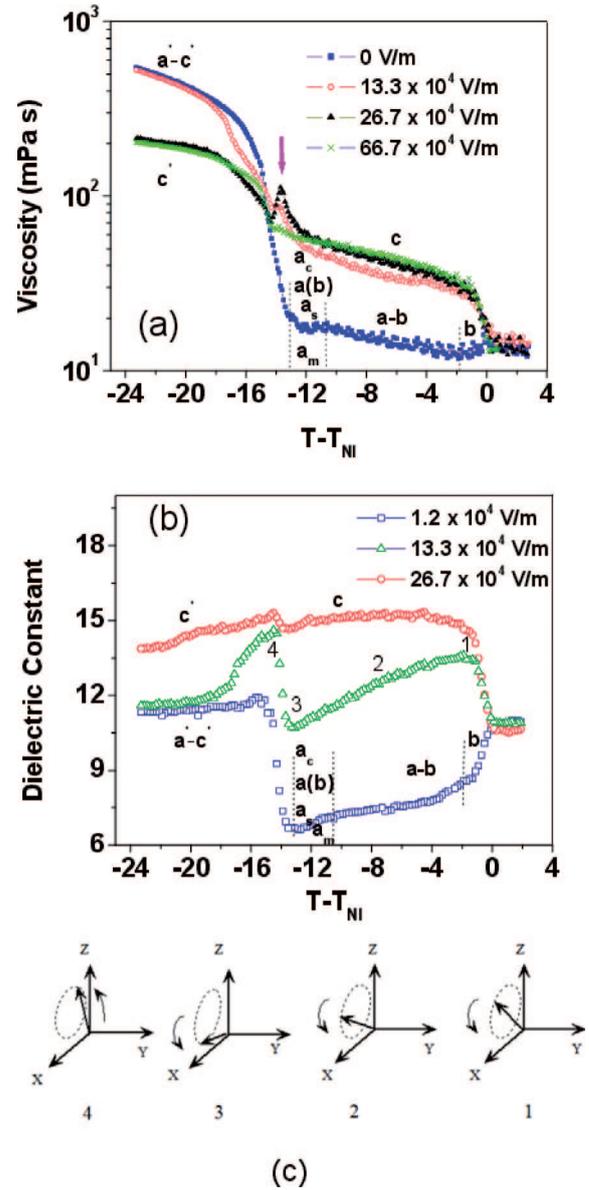
Fig. 5. (Color online) Variation of (a) the shear viscosity (η) and (b) the dielectric constant (ϵ) as a function of temperature and various applied electric fields. Vertical dotted lines are drawn considering the similarity of temperature-dependent zero-field viscosity with that of 8CB [19] and represent the approximate temperature regions with possible director orientations. The vertical arrow indicates the peak position in the viscosity ($T - T_{NI} = -13.8°$). (c) Schematic representation of the precessional motions of the director at the applied field 13.3×10^4 V/m and at various temperatures as indicated by numbers from 1 to 4 on the dielectric data in (b).

phase suggests *uniform* precessional motions of the director (below $T - T_{NI} = -2°$) about an axis (in the xz-plane) that is tilted with respect to the xy-plane. A schematic representation of the director orientation along a cone that is tilted with respect to the xy-plane is shown in fig. 5(c). The dielectric constant at 26.7×10^4 V/m in the nematic phase agrees well with $\epsilon_\parallel$ [29] at the

same temperature and indicates that at this temperature the director orients almost along the field direction and goes towards an a'-c' orientation in the SmA phase. At the applied field $\sim 26.7 \times 10^4 \, \text{V/m}$, the temperature-dependent viscosity is almost similar with the data measured at $13.3 \times 10^4 \, \text{V/m}$, except for a slight increase in the viscosity in the nematic phase and a slight increase in the peak height of the anomalous viscosity. In the SmA phase at $\sim 26.7 \times 10^4 \, \text{V/m}$ the viscosity is substantially low compared to the viscosity measured at zero field or $13.3 \times 10^4 \, \text{V/m}$. On the other hand, the dielectric data in the SmA phase at $26.7 \times 10^4 \, \text{V/m}$ is almost comparable to $\epsilon_\parallel$ as measured in the aligned cell sample [29]. This indicates that under this field the SmA layers are parallel to the shear plane and acquire c' orientation (fig. 1). Further, at higher field ($\sim 66.7 \times 10^4 \, \text{V/m}$) there is no significant change in the viscosity in the nematic and SmA phases compared to the values at $26.7 \times 10^4 \, \text{V/m}$ except that the anomalous peak is suppressed completely.

At least two possible explanations can be considered for the occurrence of the anomalous peak across the N-SmA transition. The anomalous increase of shear viscosity can occur due to the effect of shear on the pretransitional fluctuating clusters as suggested by de Gennes [30] and Onuki [31]. When the SmA phase is approached from the nematic phase the relaxation time of the collective fluctuation of smectic clusters increases and the flow field can easily distort the clusters as suggested by Safina *et al.* [15], as a result the viscosity can increase anomalously. However, the suppression of the viscosity peak at higher field cannot be understood on this basis. Another possible explanation is based on the large contribution of the Leslie coefficient α_1 to the measured viscosity. When sufficient electric field is applied the director tends to align in the field direction (z-axis). The flow alignment angle is obtained from the balance of the viscous torque and the electric torque that is given by [16,17]

$$(\alpha_3 \sin^2 \theta - \alpha_2 \cos^2 \theta)\dot{\gamma} - \frac{1}{2}\Delta\epsilon E^2 \sin 2\theta = 0, \quad (1)$$

where $\Delta\epsilon$ is the dielectric anisotropy and E is the applied electric field. The viscosity in such condition can be calculated by using Leslie-Ericksen theory [1,2]

$$\eta(\theta) = \alpha_1 \cos^2 \theta \sin^2 \theta + \frac{1}{2}(\alpha_3 + \alpha_6)\sin^2 \theta$$
$$+ \frac{1}{2}(\alpha_5 - \alpha_2)\cos^2 \theta + \frac{1}{2}\alpha_4, \quad (2)$$

where α_1 to α_6 are the Leslie coefficients [16,17]. Due to the smallness of α_1 it is neglected frequently in the nematic phase but this can contribute significantly to the measured viscosity near the N-SmA phase transition as suggested by Negita *et al.* [27]. Under zero field there are several precessional motions just above the T_{NA} which are suppressed at some finite field ($\sim 13.3 \times 10^4 \, \text{V/m}$) and the director orientation changes gradually via precessional motion around a cone as shown in fig. 5(c). In the nematic phase it starts from some finite angle on the cone (fig. 5(c)-1) and rotates from some minimum angle (fig. 5(c)-3) to a maximum angle ($\sim 90°$, fig. 5(c)-4) through $45°$ at which the first term in eq. (2) has the maximum contribution and can lead to the peak in the shear viscosity. Further, it is noticed from fig. 5(b) that at $13.3 \times 10^4 \, \text{V/m}$ the minimum (mark 3 in fig. 5(b)) and the maximum (mark 4 in fig. 5(b)) in the dielectric constant occur at temperatures $T - T_{NI} \simeq -13.3°$ and $\simeq -14.3°$, respectively. Interestingly the anomalous peak in the viscosity data (fig. 5(a)) at the same field appears at an intermediate temperature $T - T_{NI} \simeq -13.8°$ and indicates that the director orientation at the anomalous peak is nearly $45°$. When the field is sufficiently high the director is aligned parallel to the field direction and the precessional motions are completely suppressed, consequently α_1 does not contribute to η and the peak is suppressed.

In conclusion, we have measured the shear viscosity of 8OCB in both the N and SmA phases as functions of temperature and applied electric field. The flow curve at various applied fields shows the competing orientating effect of the flow field and electric field. The viscosity increases with increasing electric field in the nematic phase and saturates to η_1. At sufficiently high field the SmA exhibits c' orientation and the corresponding viscosity is significantly low compared to the viscosity of the a'-c' orientations. The shear viscosity and the dielectric data at zero or small electric field suggest the occurrence of several structures related to the precessional motions of the director as reported in 8CB. An anomalous peak is observed in the viscosity across the N-SmA transition (*i.e.* from c to c' orientation). Two possible explanations are discussed for the anomalous increase in the viscosity, namely the pretransitional smectic fluctuations and the large contribution of α_1 to the shear viscosity near T_{NA}. We argue that the second explanation is more appropriate and explains our data satisfactorily.

References

1. F.M. Leslie, J. Mech. Appl. Math. **19**, 357 (1966).
2. J.L. Ericksen, Arch. Ration. Mech. Anal. **4**, 231 (1960).
3. O. Parodi, J. Phys. (Paris) **31**, 581 (1970).
4. M. Miesowicz, Nature (London) **158**, 27 (1946).
5. M. Miesowicz, Nature (London) **17**, 261 (1935).
6. M. Miesowicz, Bull. Acad. Pol. Sci A 228 (1936).
7. Ch. Gahwiller, Phys. Lett. A **36**, 311 (1971).
8. Ch. Gahwiller, Mol. Cryst. Liq. Cryst. **20**, 301 (1973).
9. Orsay Liquid Crystal Group, Mol. Cryst. Liq. Cryst. **13**, 187 (1971).
10. W.H. de Jeu, *Physical Properties of Liquid Crystal Materials* (Gordon and Breach, New York, 1980).
11. J. Janik, J.K. Moscicki, K. Czuprynski, R. Dabrowski, Phys. Rev. E **58**, 3251 (1998).
12. P.G. de Gennes, *The Physics of Liquid Crystals*, 2nd ed. (Oxford University Press, Oxford, 1993).
13. V.V. Belyaev, *Viscosity of Nematic Liquid Crystals*, 1st Indian edition (Cambridge International Science Publishing Ltd., Cambridge, 2011).

14. R.F. Bruinsma, C.R. Safinya, Phys. Rev. A **43**, 5377 (1991).
15. C.R. Safinya, E.B. Sirota, R.J. Plano, Phys. Rev. Lett. **66**, 1986 (1991).
16. T. Carlsson, K. Skarp, Mol. Cryst. Liq. Cryst. **78**, 157 (1981).
17. T. Carlsson, K. Skarp, Mol. Cryst. Liq. Cryst. **104**, 307 (1984).
18. H. Kneppe, F. Schneirder, N.K. Sharma, J. Chem. Phys. **77**, 3203 (1982).
19. K. Negita, M. Inoue, S. Kondo, Phys. Rev. E. **74**, 051708 (2006).
20. K. Negita, H. Kaneko, Phys. Rev. E **80**, 011705 (2009).
21. J. Jadzyn, G. Czechowski, J. Phys.: Condens. Matter. **13**, L261 (2001).
22. A.G. Chmielewski, Mol. Cryst. Liq. Cryst. **132**, 339 (1986).
23. L. Ramos, M. Zapotocky, T.C. Lubensky, D.A. Weitz, Phys. Rev. E **66**, 031711 (2002).
24. K. Negita, J. Chem. Phys. **105**, 7837 (1996).
25. J. Jadzyn, G. Czechowski, Phys. Rev. A **64**, 052702 (2001).
26. H. Graf, H. Kneppe, F. Schneider, Mol. Phys. **77**, 521 (1992).
27. K. Negita, Mol. Cryst. Liq. Cryst. **300**, 163 (1997).
28. K. Negita, Int. J. Mod. Phys. B **13**, 2005 (1999).
29. J. Jadzyn, G. Czechowski, Liq. Cryst. **4**, 157 (1989).
30. P.G. de Gennes, Mol. Cryst. Liq. Cryst. **34**, 91 (1976).
31. A. Onuki, K. Kawasaki, Ann. Phys. (N.Y.) **121**, 456 (1979).
32. J. Janik, A.K. Otwinowska, Rev. Sci. Instrum. **77**, 123906 (2006).
33. A.V. Zakharov, J. Thoen, Phys. Rev. E **69**, 051709 (2004).
34. P. Pieranski, E. Guyon, Phys. Rev. Lett. **32**, 924 (1974).
35. A.V. Zakharov, A.A. Vakulenko, J. Thoen, J. Chem. Phys. **118**, 4253 (2003).
36. M.T. Cidade, C.R. Leal, P. Patricio, Liq. Cryst. **37**, 1305 (2010).